Robust Density-Based Clustering to Identify Metastable Conformational States of Proteins – Supporting Information –

Florian Sittel and Gerhard Stock
Biomolecular Dynamics, Institute of Physics,
Albert Ludwigs University, 79104 Freiburg, Germany

(Dated: April 6, 2016)

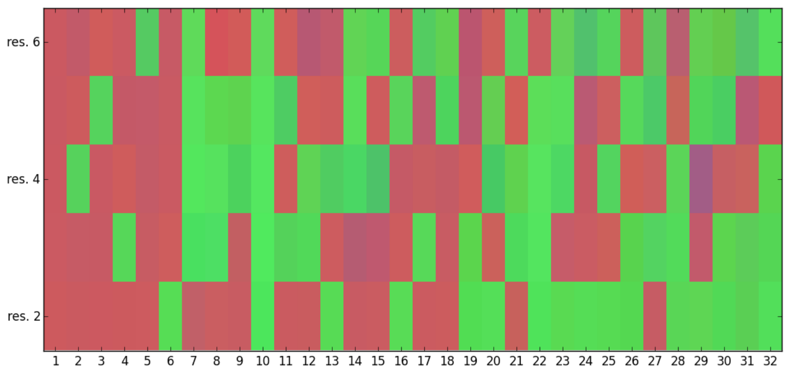

Figure S1: Ramacolor plot of Ala_7, showing the dihedral angle content of its 32 metastable states. Red residues indicate β-sheet, green residues indicate α-helical conformations.

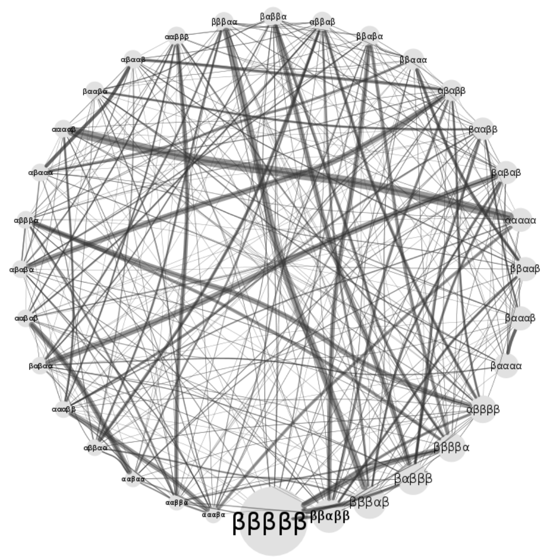

Figure S2: Transition network of Ala_7. States are ordered counter-clockwise by population. Edge-thickness scales by transition rates, node sizes correspond to state populations. Node labels denote the dihedral conformation of the state, with residues either in β- or α-conformation. The network shows clearly that Ala_7 dynamics are essentially uncorrelated.

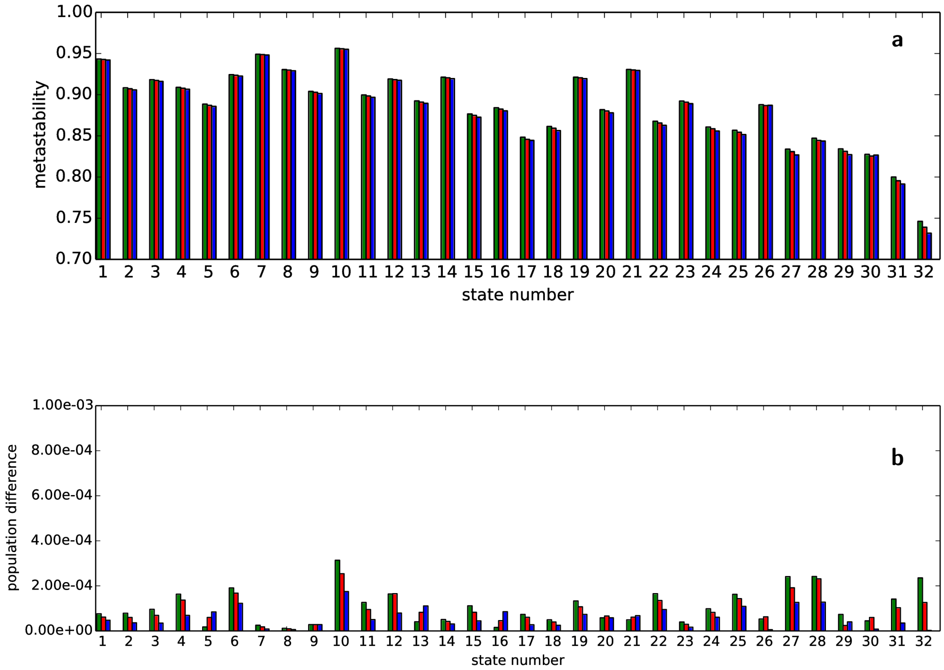

Figure S3: Verification of Chapman-Kolmogorov equation for Ala_7 . Top diagram (**a**) shows metastabilities $T_{ii}^{20\ \mathrm{ps}/\tau}(\tau)$ after propagation to 20 ps for $\tau = 1$ ps (green), $\tau = 5$ ps (red) and $\tau = 10$ ps (blue). Bottom diagram (**b**) shows differences in population after propagation of an initially equally distributed population **p**. Compared are the same lag times as in (**a**) to a propagation with $T(\tau = 20\ \mathrm{ps})$, i.e., pop. diff. $\equiv \|\mathbf{p}T^{20\ \mathrm{ps}/\tau}(\tau) - \mathbf{p}T(\tau = 20\ \mathrm{ps})\|$.

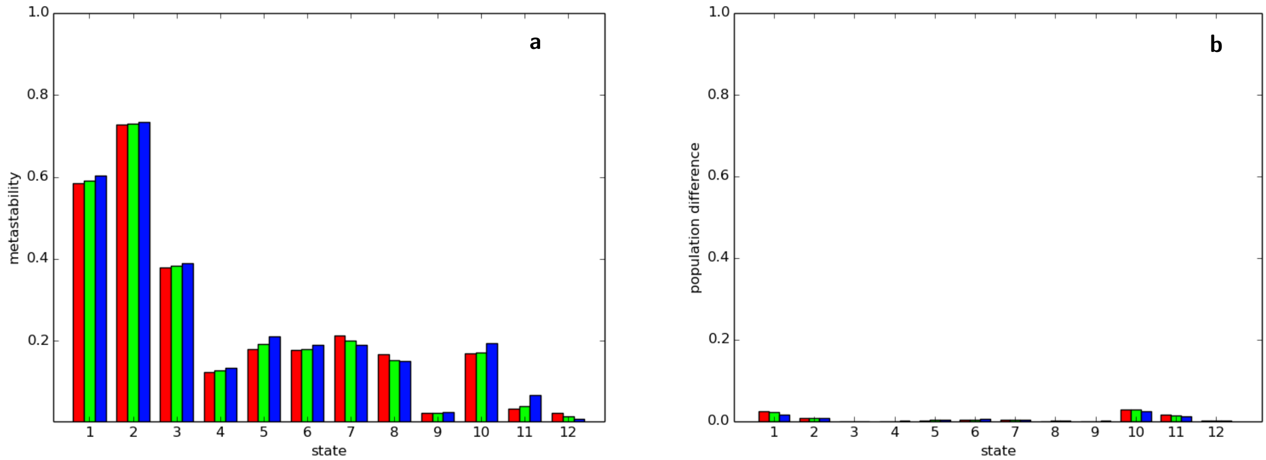

Figure S4: Verification of Chapman-Kolmogorov equation for HP-35. **a**: Metastabilities $T_{ii}^{160\ \mathrm{ns}/\tau}(\tau)$ after propagation to 160 ns for $\tau = 10$ ns (green), $\tau = 20$ ns (red) and $\tau = 40$ ns (blue). **b**: Differences (relative) in population after propagation of an initially equally distributed population **p**. Compared are the same lag times as in (**a**) to a propagation with $T(\tau = 160\ \mathrm{ns})$, i.e., pop. diff. $\equiv \|\mathbf{p}T^{160\ \mathrm{ns}/\tau}(\tau) - \mathbf{p}T(\tau = 160\ \mathrm{ns})\|$

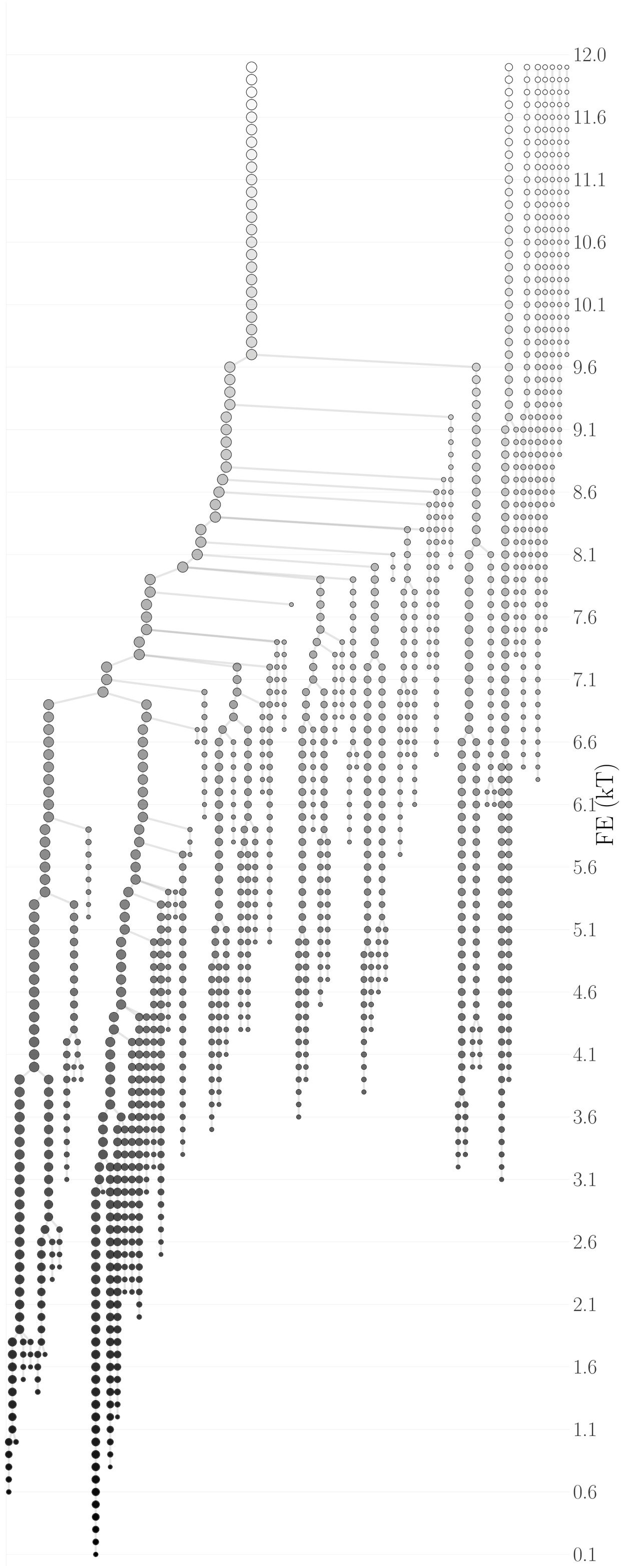

Figure S5: Density network for BPTI with free energy levels from 0.1 kT to 12.0 kT in steps of 0.1 kT.

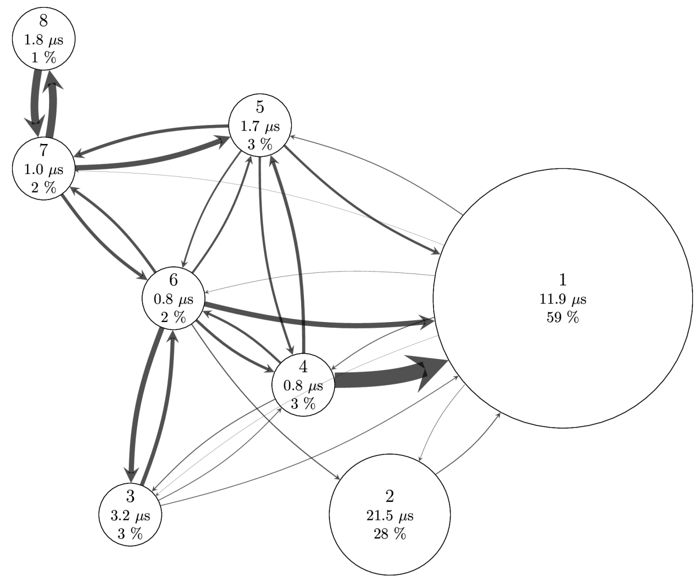

Figure S6: Markov state model of BPTI resulting from density-based geometric clustering and successive dynamical clustering via MPP on reduced dihedral-angle PCs.

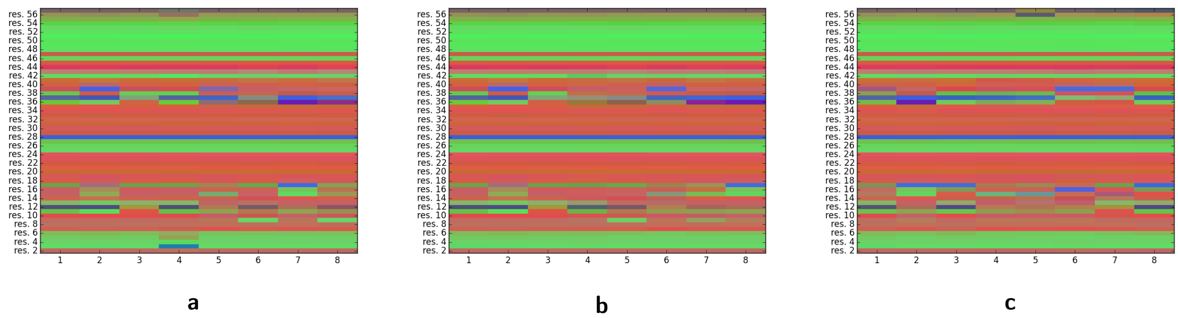

Figure S7: Dihedral angle content for BPTI after: primitive clustering (**a**), density-based geometric microstate generation and successive dynamical clustering via MPP (**b**) and density-based geometric clustering without dynamical corrections (**c**).